



The following Communications have been judged by at least two referees to be “very important papers” and will be published online at www.angewandte.org soon:

A. Müller, R. Stürmer, B. Hauer, B. Rosche*

Stereospecific Alkyne Reduction: Novel Activity of Old Yellow Enzymes

A. Wakamiya, K. Mori, S. Yamaguchi*

3-Boryl-2,2'-bithiophene as a Versatile Core Skeleton for Full-Color Highly Emissive Organic Solids

C. Defieber, M. A. Ariger, P. Moriel, E. M. Carreira*

Iridium-Catalyzed Synthesis of Primary Allylic Amines From Allylic Alcohols: Sulfamic Acid as an Ammonia Equivalent

X. Xiao, P. Yu, H.-S. Lim, D. Sikder, T. Kodadek*

A Cell-Permeable Synthetic Transcription Factor Mimic

L. C. Gontard, L.-Y. Chang, C. J. D. Hetherington, A. I. Kirkland, D. Ozkaya, R. E. Dunin-Borkowski*

Aberration-Corrected Imaging of Active Sites on Industrial Catalyst Nanoparticles

M. Königsmann, N. Donati, D. Stein, H. Schönberg, J. Harmer, A. Sreekanth, H. Grützmacher*

Metalloenzyme-Inspired Catalysis: Selective Oxidation of Primary Alcohols with Iridium Aminyl Radical Complexes

Catalysis: Prizes for Z. Hou, G. C. Fu, J. Terao, and M. C. W. Chan

News

1942

Combinatorial and High-Throughput Discovery and Optimization of Catalysts and Materials

Radislav A. Potyrailo, Wilhelm F. Maier

Books

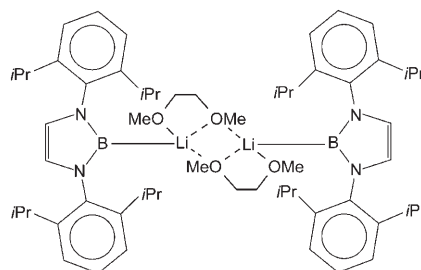
reviewed by O. Trapp 1943

Electronic Excitations in Liquefied Rare Gases

Werner F. Schmidt, Eugen Illenberger

reviewed by P. Scheier 1944

B negative: By reduction of a 2-bromo-1,3,2-diazaborole Yamashita, Nozaki, and co-workers have obtained the first three-coordinate boryl anion (see formula), which provides an unprecedented and synthetically highly useful source for a nucleophilic boron species.

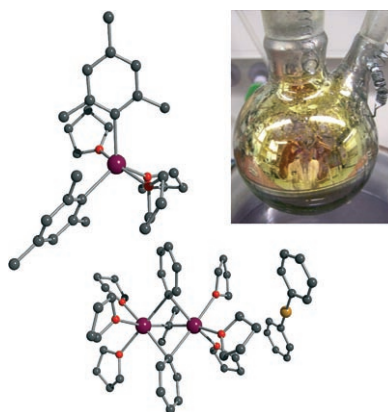


Highlights

Boryl Anions

H. Braunschweig* 1946–1948

Lithiumboryl—A Synthon for a Nucleophilic Boryl Anion



Calcium supplements for Grignard: The easy access of aryl calcium compounds in high yields now offers the possibility of investigating the properties and chemical behavior of these heavy Grignard reagents (see picture; C black, Ca purple, Cu yellow, O red). The key points are the nature of activation of the metal prior to use and the use of low reaction and handling temperatures to prevent side and decomposition reactions.

Minireviews

Heavy Grignard Reagents

M. Westerhausen,* M. Gärtner, R. Fischer, J. Langer 1950–1956

Aryl Calcium Compounds: Syntheses, Structures, Physical Properties, and Chemical Behavior

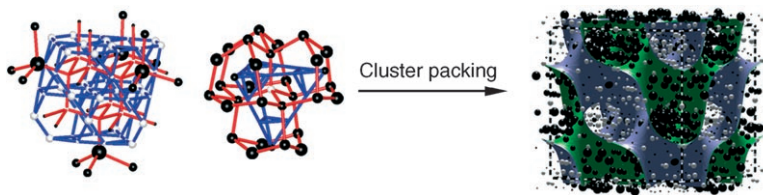
Reviews

Solid-State Structures

D. C. Fredrickson, S. Lee,*
R. Hoffmann* 1958 – 1976



Interpenetrating Polar and Nonpolar
Sublattices in Intermetallics: The NaCd₂
Structure



Inorganic, and yet more complex than an enzyme? The giant unit cells of Mg₂Al₃, NaCd₂, and Cu₄Cd₃ have challenged geometers of nature—so many beautiful polyhedra and networks to choose from. Could quantum mechanics help pick

among alternative patterns? Indeed, simple calculations highlight building blocks derived from the MgCu₂ structure type, which pack together in interpenetrating regions of polar and nonpolar bonding (see scheme for NaCd₂).

Communications

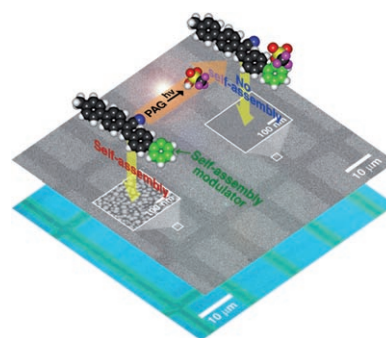
Fluorescent Nanoparticles

B.-K. An, S.-K. Kwon,
S. Y. Park* 1978 – 1982



Photopatterned Arrays of Fluorescent
Organic Nanoparticles

Bottom-up and top-down nanofabrication: A fluorescent organic molecule bearing a self-assembly modulator was assembled in situ through a vapor-driven self-assembly process into strongly fluorescent spherical nanoparticles (about 30 nm in diameter) in the photochemically delineated regions of a polymer matrix (see picture; PAG: photoacid generator).

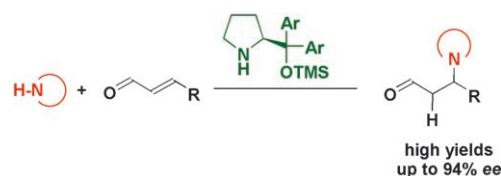


Organocatalysis

P. Dinér, M. Nielsen, M. Marigo,
K. A. Jørgensen* 1983 – 1987



Enantioselective Organocatalytic
Conjugate Addition of N Heterocycles
to α,β -Unsaturated Aldehydes



Must love cats! Chiral amines catalyze the enantioselective addition of N-heterocyclic compounds to α,β -unsaturated compounds in high yields and with enantioselectivities of up to 94% ee (see

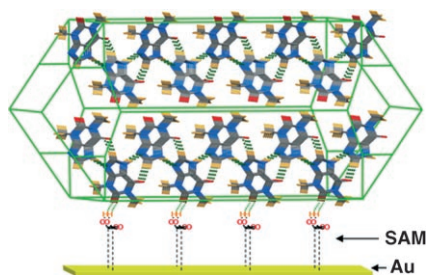
scheme; TMS = trimethylsilyl). The intermediates and transition states for the catalytic cycle were identified by performing DFT calculations.

For the USA and Canada:

ANGEWANDTE CHEMIE International Edition (ISSN 1433-7851) is published weekly by Wiley-VCH, PO Box 191161, 69451 Weinheim, Germany. Air freight and mailing in the USA by Publications Expediting Inc., 200

Meacham Ave., Elmont, NY 11003. Periodicals postage paid at Jamaica, NY 11431. US POSTMASTER: send address changes to *Angewandte Chemie*, Wiley-VCH, 111 River Street, Hoboken, NJ 07030. Annual subscription price for institutions: US\$ 5685/5168 (valid for print and

electronic / print or electronic delivery); for individuals who are personal members of a national chemical society prices are available on request. Postage and handling charges included. All prices are subject to local VAT/sales tax.



SAMs in charge: The monohydrate and anhydrous forms of theophylline crystallize concomitantly from ethanol solutions, but hydrophilic thiol self-assembled monolayers (SAMs) promote the selective growth of the anhydrous form (see picture; C gray, H yellow, N blue, O red). This selectivity is a result of interfacial hydrogen bonding and geometric epitaxy.

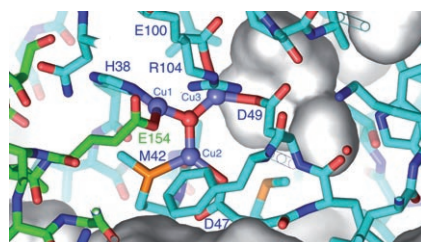
Drug Crystal Growth

J. R. Cox, M. Dabros, J. A. Shaffer, V. R. Thalladi* — 1988 – 1991

Selective Crystal Growth of the Anhydrous and Monohydrate Forms of Theophylline on Self-Assembled Monolayers



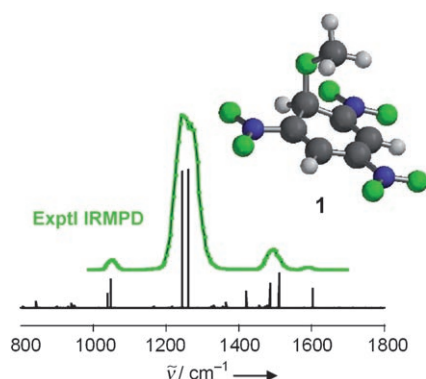
A pocketful of coppers: Redox potentiometry and EPR experiments have confirmed that the active site of the particulate methane monooxygenase (pMMO), a membrane-bound enzyme that hydroxylates methane to methanol under ambient conditions, consists of one trinuclear copper cluster (see picture) and one type 2 copper site, in addition to the dinuclear copper cluster revealed previously by X-ray crystallography.



Bioinorganic Chemistry

S. I. Chan,* V. C.-C. Wang, J. C.-H. Lai, S. S.-F. Yu, P. P.-Y. Chen, K. H.-C. Chen, C.-L. Chen, M. K. Chan — 1992 – 1994

Redox Potentiometry Studies of Particulate Methane Monooxygenase: Support for a Trinuclear Copper Cluster Active Site

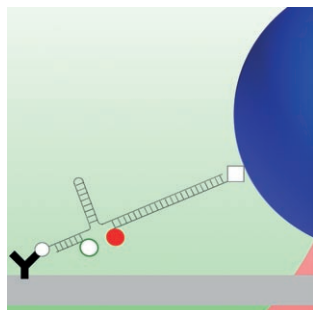


Proof positive: Infrared multiphoton dissociation (IRMPD) spectroscopy, with the tunable IR radiation of a free-electron laser source, provides positive identification of alkoxy adducts of 1,3,5-trinitrobenzene as prototypical anionic σ complexes in the gas phase (see calculated IR spectrum of **1** under the experimental IRMPD spectrum; N blue, O green, C gray, H light gray).

Gas-Phase Spectroscopy

B. Chiavarino, M. E. Crestoni, S. Fornarini,* F. Lanucara, J. Lemaire, P. Maître — 1995 – 1998

Meisenheimer Complexes Positively Characterized as Stable Intermediates in the Gas Phase



Don't FRET: The first successful combination of optical-tweezers force microscopy and single-molecule fluorescence resonant energy transfer (FRET) is demonstrated with a force sensor based on a DNA hairpin (see picture). As the hairpin is opened and closed by the optical tweezers, the structural change is simultaneously monitored by the FRET emission from fluorescence labels.

Single-Molecule Manipulation

P. B. Tarsa, R. R. Brau, M. Barch, J. M. Ferrer, Y. Freyzon, P. Matsudaira, M. J. Lang* — 1999 – 2001

Detecting Force-Induced Molecular Transitions with Fluorescence Resonant Energy Transfer

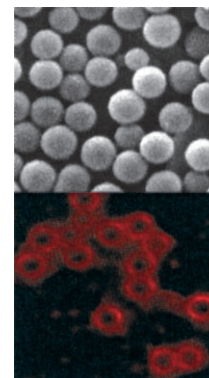
Peptide Self-Assembly

S. Ghosh, M. Reches, E. Gazit,*
S. Verma* — 2002 – 2004



Bioinspired Design of Nanocages by Self-Assembling Triskelion Peptide Elements

Winning the three-legged race: Rapid self-organization of a tripodal aromatic di-peptide conjugate on a tris(2-amino-ethyl)amine scaffold leads to a vesicular morphology (upper image). The structures can trap a fluorescent dye (lower image) and release it upon acidification, suggesting the use of such stimuli-responsive materials as potential delivery vehicles.

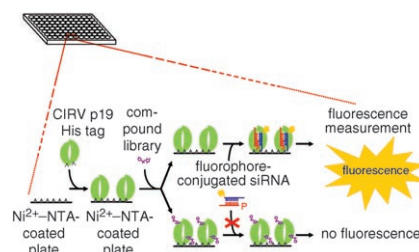


RNA-Protein Interactions

S. M. Sagan, R. Koukikolo, E. Rodgers,
N. K. Goto, J. P. Pezacki* — 2005 – 2009



Inhibition of siRNA Binding to a p19 Viral Suppressor of RNA Silencing by Cysteine Alkylation



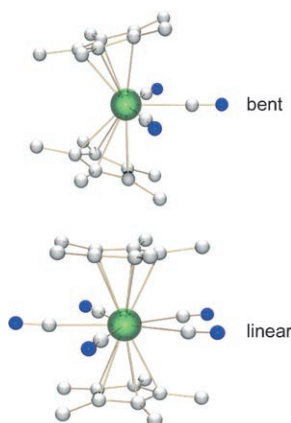
Eukaryotes have evolved complex cellular responses to double-stranded RNA. The quantities of short interfering RNA (siRNA) can be determined rapidly by using 96-well arrays of the carnation Italian ringspot virus (CIRV) p19 protein, which binds double-stranded siRNAs with nanomolar affinity and discriminates siRNA according to length. Two compounds were found to inhibit siRNA binding to CIRV p19 by alkylating active-site cysteine residues (see diagram).

Actinides

J. Maynadié, N. Barros, J.-C. Berthet,*
P. Thuéry, L. Maron,*
M. Ephritikhine* — 2010 – 2012



The Crucial Role of the f Electrons in the Bent or Linear Configuration of Uranium Cyanido Metallocenes



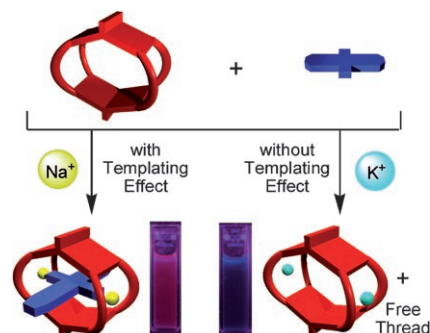
What makes it go linear? The synthesis of the first polycyanide compounds of a 5f element (see picture, U green, N blue, C white) supports the idea that the geometry of metallocenes depends on both the metal oxidation state and the size and shape of the equatorial ligands. Theoretical investigations reveal that the stability of these novel linear π -sandwich compounds is determined by the availability of f orbitals.

Host-Guest Chemistry

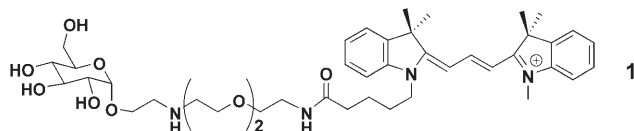
S.-Y. Hsueh, C.-C. Lai, Y.-H. Liu,
S.-M. Peng, S.-H. Chiu* — 2013 – 2017



Highly Selective Na⁺-Templated Formation of [2]Pseudorotaxanes Exhibiting Significant Optical Outputs



The chosen one: A molecular cage has been shown to form pseudorotaxane-like complexes with threaded anthraquinone and squaraine units in the presence of templating Na⁺ ions (see picture). The complexation and decomplexation of the pseudorotaxane complexes in solution occur with significant color changes which allows this ion-specific templating effect to be easily monitored with the naked eye.



Tracing glucose uptake: Fluorescent glucose analogues were synthesized, and the importance of stereochemistry for cellular uptake efficiency was demonstrated. The chiral bioprobe **1** showed superior properties as a glucose-uptake tracer. The

cellular uptake of **1** was demonstrated under various concentrations of D-glucose. A screening system was developed for the discovery of anticancer agents by the measurement of glucose uptake in cancer cells with **1**.

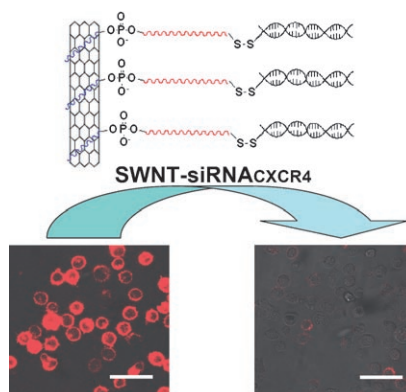
Fluorescent Bioprobes

J. Park, H. Y. Lee, M.-H. Cho,
S. B. Park* 2018–2022

Development of a Cy3-Labeled Glucose Bioprobe and Its Application in Bioimaging and Screening for Anticancer Agents



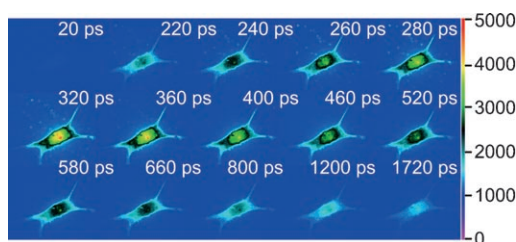
Special delivery: Functionalized single-walled nanotubes (SWNT) can be used as molecular transporters to shuttle short interfering RNA (siRNA) into human T cells and primary cells and silence the expression of HIV-specific cell-surface receptors and coreceptors (see picture; scale bars 40 μm). This silencing effect, known to block HIV viral entry and reduce infection, is superior to that observed with conventional liposome-based nonviral delivery agents.



Nanobiotechnology

Z. Liu, M. Winters, M. Holodniy,
H. Dai* 2023–2027

siRNA Delivery into Human T Cells and Primary Cells with Carbon-Nanotube Transporters



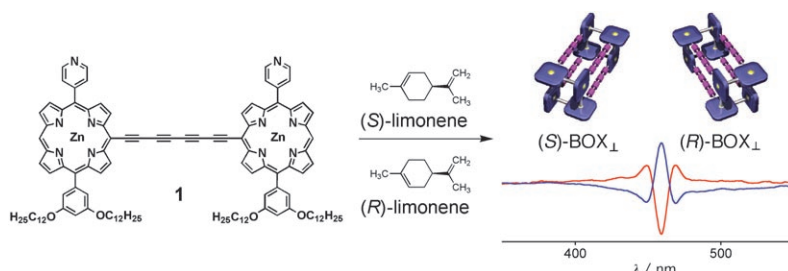
Every nucleolus has a silver lining: Formation of silver nanoclusters by fluorescence photoactivation was used for the staining of cells at low silver nitrate

concentrations and ambient temperature. The picture shows picosecond lifetime images of peptide-encapsulated silver nanoclusters within NIH 3T3 cells.

Cell Staining

J. Yu, S. A. Patel,
R. M. Dickson* 2028–2030

In Vitro and Intracellular Production of Peptide-Encapsulated Fluorescent Silver Nanoclusters



The surrounding shapes the box: The zinc porphyrin dimer **1** bearing pyridyl groups can chiroptically sense an asymmetric hydrocarbon, such as limonene, by forming the homochiral box-shaped tetrameric

assembly BOX_⊥. As the BOX_⊥ formed is enantiomerically enriched, the optical purity as well as the absolute configuration of the solvent limonene can be determined.

Molecular Recognition

J. Aimi, K. Oya, A. Tsuda,*
T. Aida* 2031–2035

Chiroptical Sensing of Asymmetric Hydrocarbons Using a Homochiral Supramolecular Box from a Bismetalloporphyrin Rotamer

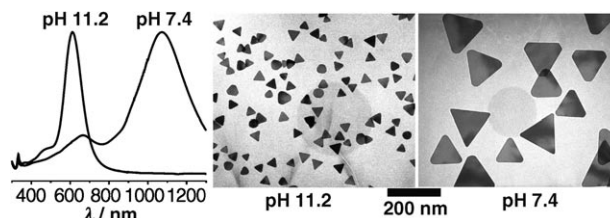


Nanoparticle Growth

C. Xue, C. A. Mirkin* — 2036–2038



pH-Switchable Silver Nanoprism Growth Pathways



A pHunction of pH: The silver nanoprism fusion process can be turned on and off as a function of the pH value during photochemical synthesis. With appropriate pH regulation (see TEM images, middle and right), one can achieve excellent control

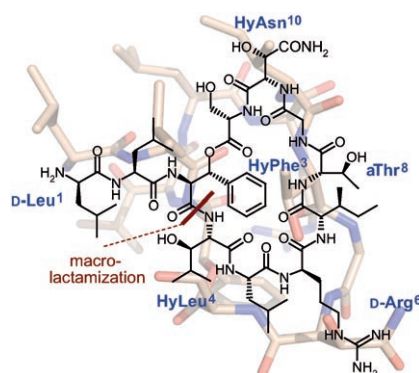
over the nanoprism edge length with a fixed 10-nm thickness and the corresponding plasmon bands, which span the visible and NIR range (see extinction spectra, left).

Antibiotic Resistance

F. von Nussbaum,* S. Anlauf, J. Benet-Buchholz, D. Häbich, J. Köbberling, L. Musza, J. Telser, H. Rübsamen-Waigmann, N. A. Brunner — 2039–2042



Structure and Total Synthesis of Lysobactin (Katanosin B)



Tackle-resistant bacteria: Determination of the 3D structure of the antibiotic lysobactin has led to its total synthesis and resulted in a high-yielding macrolactamization step. The minimal use of protecting groups allowed preorganization of the side chains to steer the cyclization. Thus, a new chemical route has been developed in the search for innovative antibiotic lead structures.

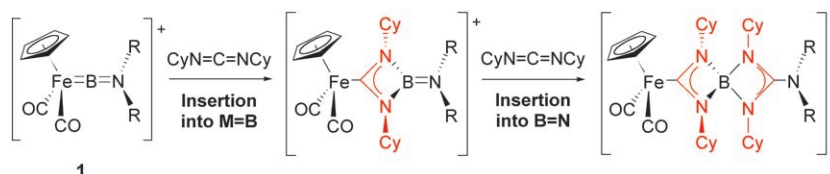


Borylene Complexes

G. A. Pierce, S. Aldridge,* C. Jones, T. Gans-Eichler, A. Stasch, N. D. Coombs, D. J. Willock — 2043–2046



Cationic Terminal Aminoborylene Complexes: Controlled Stepwise Insertion into M=B and B=N Double Bonds



One thing leads to another: Reactions of the cationic BN vinylidene analogues **1** [BAr^F₄] (R = Cy, *i*Pr; Ar^F = 3,5-(CF₃)₂C₆H₃) towards dicyclohexylcarbodiimide proceed by unprecedented insertion chemistry for terminal borylene complexes. Con-

trolled, stepwise insertion into the Fe=B and B=N bonds is demonstrated, sequentially forming four-membered rings linked at a spirocyclic boronium center.

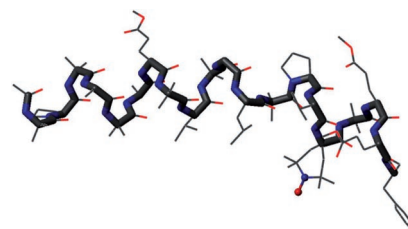
Peptide Structures

M. Crisma,* C. Peggion, C. Baldini, E. J. MacLean, N. Vedovato, G. Rispoli, C. Toniolo — 2047–2050

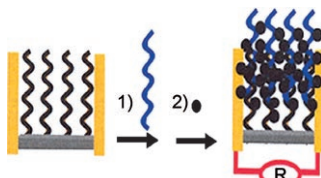


Crystal Structure of a Spin-Labeled, Channel-Forming Alamethicin Analogue

Crystal clear: A detailed conformational characterization of a synthetic analogue of the peptide antibiotic alamethicin (see structure; C gray, N blue, O red) has been achieved by X-ray diffraction. The high-resolution structure of this analogue, which incorporates a spin probe, paves the way for a better understanding of the mode of action of alamethicin.



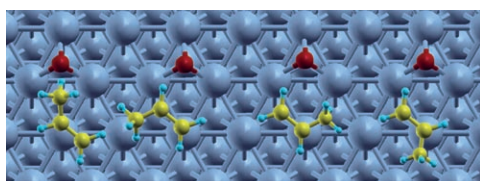
Build a bridge: Strong interactions between zirconium-activated indium tin oxide (ITO) nanoparticles and phosphates are utilized to label nucleic acids with multiple ITO nanoparticles under very mild conditions. The electrically conductive ITO nanoparticle network formed bridges the gap between a pair of interdigitated electrodes, allowing the detection of nucleic acids at subpicomolar levels with high specificity.



Biosensors

Y. Fan, X. Chen, J. Kong, C.-h. Tung, Z. Gao* — 2051 – 2054

Direct Detection of Nucleic Acids by Tagging Phosphates on Their Backbones with Conductive Nanoparticles



Gotta have copper: DFT studies indicate that the performance of heterogeneous epoxidation catalysts depends on the first step in the reaction between oxygen atoms and propylene molecules coadsorbed on the metal surface (see picture;

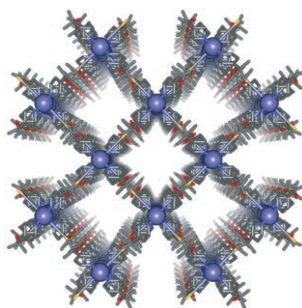
C yellow, H light blue, O red). The high basicity of oxygen atoms on silver favors allylic hydrogen stripping, whereas the low basicity of oxygen atoms on copper favors metallacycle formation and subsequent epoxidation.

Heterogeneous Catalysis

D. Torres, N. Lopez,* F. Illas, R. M. Lambert — 2055 – 2058

Low-Basicity Oxygen Atoms: A Key in the Search for Propylene Epoxidation Catalysts

Influential guests: An abrupt spin-cross-over transition is exhibited by a nanoporous framework material that consists of interpenetrated two-dimensional grids linked by hydrogen-bonding interactions. Desorption of guest molecules from the highly robust host lattice occurs by a single-crystal-to-single-crystal transformation and leads to subtle changes in the framework structure and spin-crossover properties.

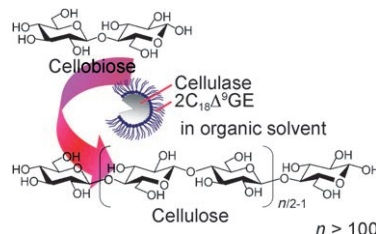


Spin Crossover

S. M. Neville, B. Moubaraki, K. S. Murray, C. J. Kepert* — 2059 – 2062

A Thermal Spin Transition in a Nanoporous Iron(II) Coordination Framework Material

High and dry: The synthesis in vitro of longer-chain cellulose with more than 100 anhydrous glucopyranose units in the polymer has been performed by a new technique for glycosynthesis. This method uses enzymatic polymerization with enzyme/surfactant complexes that act in nonaqueous organic media.



Nonaqueous Biocatalysis

S. Egusa, T. Kitaoka,* M. Goto, H. Wariishi — 2063 – 2065

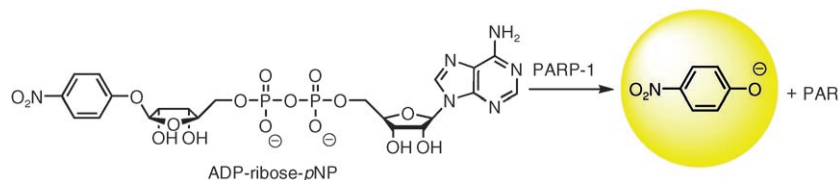
Synthesis of Cellulose In Vitro by Using a Cellulase/Surfactant Complex in a Nonaqueous Medium

Enzyme Kinetics

A. C. Nottbohm, R. S. Dothager,
K. S. Putt, M. T. Hoyt,
P. J. Hergenrother* — 2066–2069



A Colorimetric Substrate for Poly(ADP-Ribose) Polymerase-1, VPARP, and Tankyrase-1



Color me yellow: Poly(ADP-ribose) polymerases (PARPs) play a major role in cellular survival and maintenance of energy stores after genotoxic insult. The colorimetric PARP substrate ADP-ribose-*p*NP can be used to monitor PARP activity.

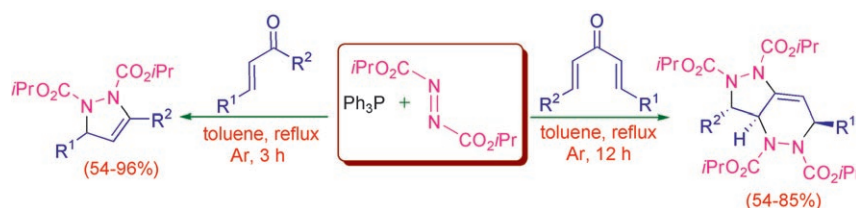
By monitoring the production of *p*-nitrophenolate, the kinetic parameters of PARP-1, tankyrase, and PARP-4 could be evaluated. ADP = adenosine diphosphate, *p*NP = *p*-nitrophenoxo.

Huisgen Zwitterions

V. Nair,* S. C. Mathew, A. T. Biju,
E. Suresh — 2070–2073



A Novel Reaction of the “Huisgen Zwitterion” with Chalcones and Dienones: An Efficient Strategy for the Synthesis of Pyrazoline and Pyrazolopyridazine Derivatives



Two unexpected transformations: The reaction of the Huisgen zwitterion derived from triphenylphosphane and diisopropyl azodicarboxylate (DIAD) with chalcones affords functionalized pyrazolines. In

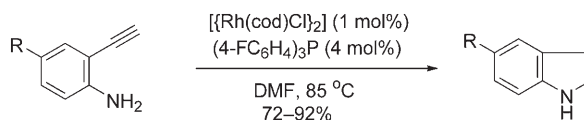
contrast, the reaction with dienones affords pyrazolopyridazines, presumably by Diels–Alder reaction of the initially formed pyrazoline with excess DIAD (see scheme).

Vinylidenes

B. M. Trost,* A. McClory — 2074–2077



Rhodium-Catalyzed Cycloisomerization: Formation of Indoles, Benzofurans, and Enol Lactones



Internal affairs: Indoles, benzofurans, and enol lactones are formed chemoselectively from the rhodium-catalyzed cycloisomerization reaction of easily prepared alkynyl aniline substrates (see scheme, cod = cycloocta-1,5-diene, DMF = *N,N*-

dimethylformamide). The reaction may proceed by nucleophilic capture of a vinylidene intermediate. Indoles are formed under mild conditions using low catalyst loadings.

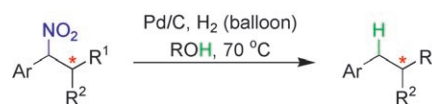
Organic Synthesis

T. C. Fessard, H. Motoyoshi,
E. M. Carreira* — 2078–2081



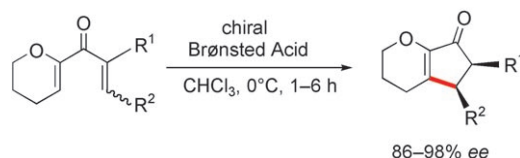
Pd-Catalyzed Cleavage of Benzylic Nitro Bonds: New Opportunities for Asymmetric Synthesis

Without a trace: Benzylic nitroalkanes are reduced to the corresponding parent alkanes in good yields by using a simple procedure involving heterolytic C–N bond cleavage (see scheme). Traceless removal of the nitro group leaves behind a stereogenic center that may otherwise be difficult to install. This reaction significantly expands the scope of building blocks that can be accessed.



Organocatalysis

M. Rueping,* W. Ieawsuwan,
A. P. Antonchick,
B. J. Nachtsheim ——— 2097–2100



Chiral Brønsted Acids in the Catalytic Asymmetric Nazarov Cyclization—The First Enantioselective Organocatalytic Electrocyclic Reaction

Low catalyst loadings, high enantioselectivities, mild conditions, and fast reaction times are the important features of the first enantioselective organocatalytic electrocyclic reaction: a Nazarov cyclization leading to the synthesis of substi-

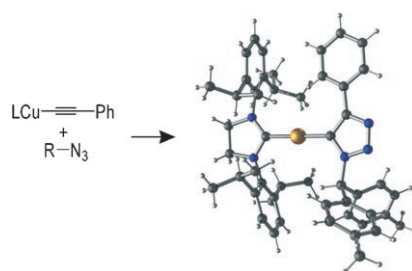
tuted five-membered rings with a chiral Brønsted acid as a catalyst (see scheme). A further advantage of this method is the possible entry to all four diastereomers of the product.

Click Intermediate

C. Nolte, P. Mayer,
B. F. Straub* ——— 2101–2103



Isolation of a Copper(I) Triazolidine: A “Click” Intermediate



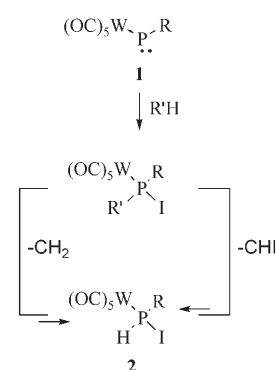
Click snapshot: In an aprotic medium, a copper(I) triazolidine complex is synthesized from a sterically hindered copper acetylide and an organoazide (see scheme: yellow Cu, blue N, dark gray C, gray H). This result provides direct evidence for such a complex, which had previously been hypothesized.

Dehydroiodination

A. Özbolet, A. A. Khan, G. von Frantzius,
M. Nieger, R. Streubel* ——— 2104–2107

Dehydroiodination of Iodo- and Diiodomethane by a Transient Phosphenidene Complex

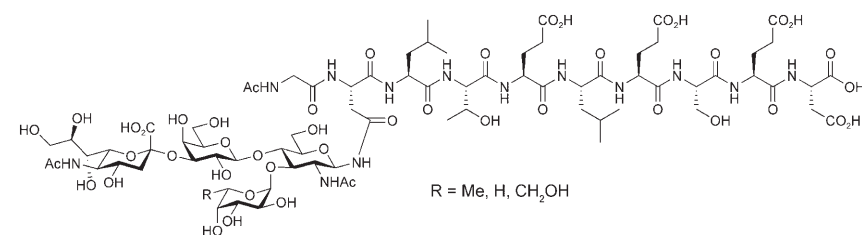
Elimination round: Dehydroiodination occurs when transient phosphinidene complex **1** is treated with iodomethane and diiodomethane, thus formally eliminating CH₂ and CHI and giving in both cases complex **2** (see scheme; R = CH-(SiMe₃)₂; R' = CH₃, CH₂I). The overall reactions represent examples of unprecedented P–C bond-cleavage reactions, and proceed under unusually mild conditions.



Better than Nature

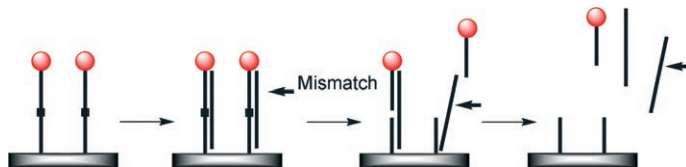
C. Filser, D. Kowalczyk, C. Jones,
M. K. Wild, U. Ipe, D. Vestweber,
H. Kunz* ——— 2108–2111

Synthetic Glycopeptides from the E-Selectin Ligand 1 with Varied Sialyl Lewis^x Structure as Cell-Adhesion Inhibitors of E-Selectin



Cooperation is key: Peptide and saccharide portions cooperate in sialyl Lewis^x glycopeptides and their mimetics in the fucose and sialic acid parts (see formula), resulting in up to greater than 100-fold stronger binding to E-selectin. The synth-

esis provided sialyl Lewis^x amino acids in a form sufficiently acid-stable for application in automated solid-phase syntheses of glycopeptides based on acid-sensitive linkers.



Game, set, and mismatch: In a new method for the detection of base-pair mismatches, an immobilized DNA strand with a cleavage site (black square) and a detection tag (red circle) is hybridized

with the target strand. If the target nucleotide has a mismatch, then the marker is released from the solid phase (see scheme).

Analytical Methods

S. Thoeni, C. J. Kressler,
B. Giese* _____ 2112–2114

Site-Specific DNA Cleavage on a Solid Support: A Method for Mismatch Detection



Supporting information is available on the WWW (see article for access details).



A video clip is available as Supporting Information on the WWW (see article for access details).

Angewandte InterScience®
DISCOVER SOMETHING GREAT

“Hot Papers” are chosen by the Editors for their importance in a rapidly evolving field of high current interest. A preview with the graphical abstracts of these articles can be found on the *Angewandte Chemie* homepage in Wiley InterScience at www.angewandte.org.

All articles in *Angewandte Chemie* are published online several weeks ahead of print. They are found under the “EarlyView” link on the journal’s homepage in Wiley InterScience.

Service

Keywords _____ 2118

Authors _____ 2119

Angewandte's
Sister Journals _____ 2116–2117

Preview _____ 2121

Corrigendum

The authors wish to cite an additional paper. In 2002, Doris and co-workers reported the reduction of α,β -unsaturated ketones in the presence of $[\text{Cp}_2\text{TiCl}]$ and MeOH via free-radical chemistry. This observation is closely related to that reported by the authors the same year on the reduction of carbon radicals in the presence of $[\text{Cp}_2\text{TiCl}]$ and water but was not cited in the present article. The authors apologize for the oversight. Reference [4] should therefore read as follows:

- [4] a) A. F. Barrero, J. E. Oltra, J. M. Cuerva, A. Rosales, *J. Org. Chem.* **2002**, 67, 2566–2571;
b) for related observations on the reduction of α,β -unsaturated ketones in the presence of $[\text{Cp}_2\text{TiCl}]$ and MeOH, see: L. Moisan, C. Hardouin, B. Rousseau, E. Doris, *Tetrahedron Lett.* **2002**, 43, 2013–2015.

Water: The Ideal Hydrogen-Atom Source in Free-Radical Chemistry Mediated by Ti^{III} and Other Single-Electron-Transfer Metals?

J. M. Cuerva,* A. G. Campaña, J. Justicia, A. Rosales, J. L. Oller-López, R. Robles, D. J. Cárdenas,* E. Buñuel, J. E. Oltra* _____ 5522–5526

Angew. Chem. Int. Ed. **2006**, 45

DOI 10.1002/anie.200600831